

Vegetation Structure from Polarimetric Interferometry

Robert N. Treuhaft and Shane R. Cloude

Corresponding author:

Robert N. Treuhaft

Jet Propulsion Laboratory, MS300-227

California Institute of Technology

4800 Oak Grove Drive

Pasadena, CA 91109

email: rnt@radar-sci.jpl.nasa.gov

Tel. 818-354-6216 Fax 818-393-5285

Shane R. Cloude

Applied Electromagnetics

11 Bell St., St. Andrews, KY16 9UR, UK

e-mail : scloude@fges.demon.co.uk

Tel/Fax: (44) (0)1334 477598/475570

Abstract

Polarimetric radar interferometry is much more sensitive to the distribution of oriented objects in a vegetated land surface than either polarimetry or interferometry alone. This paper shows that single-baseline polarimetric interferometry can be used to estimate vegetation heights and underlying topography, while at least two baselines are needed for randomly oriented volumes. Single-baseline, calculated vegetation height accuracies are in the range of 2-8 m, for levels of vegetation orientation in forests.

I. Introduction

The structure of vegetation is an important indicator of ecosystem dynamics, and enables the modeling and monitoring of ecological change [1]. This communication focuses on the measurement of the structure of vegetation by polarimetric interferometric synthetic aperture radar, called polarimetric interferometry [2]. Radar interferometry is primarily sensitive to the spatial distribution of vegetation [3] while polarimetry is primarily sensitive to the shape and orientation of vegetation scatterers [4,5]. Polarimetric interferometry, which is interferometry between all possible polarization channels at each end of the baseline, is therefore sensitive to the distribution of oriented scatterers. This communication demonstrates the enhanced capability and accuracy of polarimetric interferometry for estimating vegetation structural attributes, relative to either interferometry or polarimetry alone. The

demonstration focuses on the determination of the height of oriented vegetation volumes with polarimetric interferometry.

Many vegetated land surfaces contain a substantial volume of scatterers, for example the leaves, branches, and trunks of forests. Scattering from the volume often generates a dominant radar return. The number density of volume scatterers will depend on scatterer orientation for many vegetation volumes. Forests can have a vertically oriented component due to tree trunks and other components, such as branch layers, oriented in other directions. Crops can similarly have pronounced orientation characteristics. In order to demonstrate the applicability of polarimetric interferometry, the vegetation layer will therefore be taken to be an oriented volume, one in which the number density of scatterers depends on scatterer orientation. It will be shown that the determination of the simplest vertical structure parameters, the vegetation height and the altitude of the bottom surface (topography), is substantially improved by measuring the oriented nature of the vegetation with polarimetric interferometry.

The plan of this communication is as follows: Section II contains a description of the determination of vegetation height and surface topography in randomly oriented vegetation with interferometry only. This section shows that at least two interferometric baselines are needed when polarimetry plays no role (because the vegetation is considered to be randomly oriented). Section III treats oriented vegetation, showing that the sensitivity of fully polarimetric interferometry to spatial and orientation characteristics enables height and topography determination with a single baseline. Polarimetric interferometry also enhances multibaseline determinations. Section IV contains a summary and indicates the role of polarimetric interferometry in determining the structure of oriented volumes with oriented underlying surfaces, which describe a larger group of vegetated land surfaces.

II. The Structure of Randomly Oriented Volumes from Interferometry

A “randomly oriented volume” is one in which the number density of scatterers does *not* depend on scatterer orientation. The height and topography of a randomly oriented volume can be measured by single-polarization interferometry [3]. The introduction of polarimetry or polarimetric interferometry would bear on the measurement of average scatterer shape, but, because the scatterers have no preferred direction, would not enhance height and topography determinations [6]. In order to formulate height and topography estimation of randomly oriented vegetation, the dependence of the complex interferometric cross-correlation

on vegetation height and underlying topography is given in [3] as

$$\frac{\langle E(\vec{R}_1)E^*(\vec{R}_2) \rangle}{\sqrt{\langle E^2(\vec{R}_1) \rangle \langle E^2(\vec{R}_2) \rangle}} \propto e^{i\phi_0(z_0)} \int_0^{h_v} e^{i\alpha_z z} \exp\left[-\frac{2\sigma_x(h_v - z)}{\cos \theta_0}\right] dz \quad (1)$$

where θ_0 is the radar incidence angle, \vec{R}_1 and \vec{R}_2 are the radar receivers which form the interferometric baseline, and $E(\vec{R}_1)$ and $E(\vec{R}_2)$ are the signals derived from the received fields at each end. The quantity α_z is the derivative of interferometric phase with respect to vertical location of the scatterer, and is proportional to the interferometer baseline/(wavelength \times altitude above the surface). The cross-correlation in (1), assumes that the vegetation layer is horizontal (slope of layer=0). The vegetation parameters on which the cross-correlation in (1) depend are 1) the vegetation height, (h_v), 2) the altitude of the bottom of the vegetation layer (z_0 , the argument of the interferometric phase $\phi_0(z_0)$ at the bottom of the layer), and 3) the extinction coefficient (σ_x).

A schematic inversion of (1) for h_v and z_0 can be written as

$$\begin{pmatrix} h_v \\ z_0 \\ \sigma_x \end{pmatrix} = M^{-1} \begin{pmatrix} A \\ \phi \end{pmatrix} \quad (2)$$

where A is the amplitude of (1) and ϕ is its argument, the interferometric phase. Because the number of parameters on the left is greater than the number of observations on the right, (2) shows that a single baseline cannot be used to estimate height and topography. In practice, low-accuracy *a priori* knowledge of topography can be used to constrain (2) and invert for the three parameters, but the accuracies are poor, in the 10-m range for height. If two or more baselines are used, there are a sufficient number of interferometric amplitudes and phases to estimate the structure parameters and the extinction coefficient. For TOPSAR experimental conditions [5] at C-band, using 2.5-m and 5-m baselines, vegetation height accuracies between 6 and 8 meters have been demonstrated [6]. Improved accuracies can be expected from longer baseline pairs [7]. It will be shown below (1) no longer applies for oriented vegetation volumes, but that introduction of polarimetric interferometry enables the estimation of h_v , z_0 , and extinction properties, with a single baseline and potentially with substantial increases in parameter estimate accuracy.

III. The Structure of Oriented Volumes from Polarimetric Interferometry

If the volume is oriented, incident waves propagate along polarizations determined by the eigenvectors of the average forward-scattering matrix [8], called eigenpolarizations \hat{p}_a and \hat{p}_b . A wave polarized in the \hat{p}_a direction, for example, will remain polarized in the \hat{p}_a direction as it propagates with refractivity (index of refraction -1) χ_a and extinction σ_{x_a} , as indicated schematically in Figure 1. The cross-correlation for the oriented volume, no longer given by (1), instead can be written as [6]

$$\frac{\langle E(\vec{R}_1)E^*(\vec{R}_2) \rangle}{\sqrt{\langle E^2(\vec{R}_1) \rangle \langle E^2(\vec{R}_2) \rangle}} \propto e^{i\phi_0(z_0)} \int_0^{h_v} dz e^{i\alpha_z z} \\ \times \sum_{i,j,k,l} f_{i,j,k,l} \exp[i(\chi_i + \chi_j - \chi_k - \chi_l) \frac{(h_v - z)}{\cos \theta_0}] \exp[-\frac{\sigma_{x_i} + \sigma_{x_j} + \sigma_{x_k} + \sigma_{x_l}}{2} \frac{(h_v - z)}{\cos \theta_0}] \quad (3)$$

where each of the subscripts i, j, k, l can take on the values a and b , appropriate to the first or second eigenvalue, respectively. The terms $f_{i,j,k,l}$ involve projections of the transmit and receive interferometer polarization (both V in the case of TOPSAR) on \hat{p}_a and \hat{p}_b . The $f_{i,j,k,l}$'s also contain averaged products of the i, j and k, l elements of the complex backscattering matrix of the volume scatterers. The cross-correlation for the oriented volume therefore contains, in addition to the three parameters shown in (2), more than 20 new parameters describing the eigenpolarization propagation and the backscattering matrix products. However, if, for example, the interferometer were operated at transmit-receive polarization \hat{p}_a at both ends, then only the $i = j = k = l$ term would survive, (3) would be reduced to (1), and it would depend only on h_v , z_0 , and σ_{x_a} , which would constitute a tremendous simplification facilitating parameter estimation.

Polarimetric interferometry, represented by the polarimetric interferometric coherence, can be used to both find the eigenpolarizations of the volume and constrain the parameter set. It will be shown that polarimetric interferometry enables the reduction of the > 20 parameters in (3) to just four, which will enable a single-baseline determination of h_v and z_0 . The polarimetric interferometric coherence, which replaces the cross-correlation in (1), is given by [2]

$$\gamma \equiv \frac{\underline{w}_1^\dagger \Omega_{12} \underline{w}_2}{\sqrt{\underline{w}_1^\dagger T_{11} \underline{w}_1 \underline{w}_2^\dagger T_{22} \underline{w}_2}} \quad (4)$$

where the elements of the complex vector \underline{w}_1 specify the transmit-receive polarization combination at end 1 of the baseline, and similarly for \underline{w}_2 . The elements of the \underline{w}_i unitary

vectors are taken to be in the Pauli basis [9], for example:

$$\begin{aligned} \underline{w}_1 \text{ basis} &\equiv \begin{pmatrix} S_{HH_1} + S_{VV_1} \\ S_{VV_1} - S_{HH_1} \\ 2S_{HV_1} \end{pmatrix} \Rightarrow \\ \underline{w}_{1HH} &= \frac{1}{\sqrt{2}} \begin{pmatrix} 1 \\ -1 \\ 0 \end{pmatrix}, \quad \underline{w}_{1VV} = \frac{1}{\sqrt{2}} \begin{pmatrix} 1 \\ 1 \\ 0 \end{pmatrix}, \quad \underline{w}_{1HV} = \begin{pmatrix} 0 \\ 0 \\ 1 \end{pmatrix} \end{aligned} \quad (5)$$

where S_{HH_1} is the HH scattering matrix element at end 1 of the baseline. In (4), the Ω_{12} matrix is formed from the polarimetric scattering matrices at each end of the baseline, and for the oriented volume is given by

$$\begin{aligned} \Omega_{12} &\equiv \begin{pmatrix} S_{HH_1} + S_{VV_1} \\ S_{VV_1} - S_{HH_1} \\ 2S_{HV_1} \end{pmatrix} \begin{pmatrix} S_{HH_2} + S_{VV_2}, & S_{VV_2} - S_{HH_2}, & 2S_{HV_2} \end{pmatrix}^* \propto \\ &e^{i\phi_0(z_0)} R(2\theta) \left\{ \int_0^{h_v} e^{i\alpha_z z} \exp\left[-\frac{(\sigma_{x_1} + \sigma_{x_2})(h_v - z)}{\cos \theta_0}\right] P(\tau) \langle T_c \rangle P(-\tau) dz \right\} R(-2\theta) \end{aligned} \quad (6)$$

The expression in (6), inserted into (4), leads to coherences equivalent to (3). In (6), $\langle T_c \rangle$ is the average polarimetric coherency matrix for the oriented volume in the Pauli \hat{p}_a - \hat{p}_b basis, as opposed to the Pauli H-V basis. If reflection symmetry about the \hat{p}_a axis is assumed, $\langle T_c \rangle$ has the form [9]

$$\langle T_c \rangle \equiv \begin{pmatrix} t_{11} & t_{12} & 0 \\ t_{12}^* & t_{22} & 0 \\ 0 & 0 & t_{33} \end{pmatrix} \quad (7)$$

and $P(\tau)$ accounts for the differences in propagation characteristics of the eigenpolarizations:

$$P(\tau) \equiv \begin{pmatrix} \cosh \tau & \sinh \tau & 0 \\ \sinh \tau & \cosh \tau & 0 \\ 0 & 0 & 1 \end{pmatrix} \quad (8)$$

where

$$\tau \equiv (\sigma_{x_a} - \sigma_{x_b} + i(\chi_a - \chi_b)) \frac{h_v - z}{\cos \theta_0} \quad (9)$$

The rotation matrix $R(2\theta)$ between the Pauli \hat{p}_a - \hat{p}_b basis and the Pauli H-V basis is given by

$$R(2\theta) \equiv \begin{pmatrix} 1 & 0 & 0 \\ 0 & \cos 2\theta & \sin 2\theta \\ 0 & -\sin 2\theta & \cos 2\theta \end{pmatrix} \quad (10)$$

where θ is the angle between the eigenpolarization vector \hat{p}_a and the horizontal, H axis (i.e. if the eigenpolarizations were H and V, θ would be zero). In (6), T_{11} and T_{22} , which

are the polarimetric coherences at each end of the baseline, are equal (in the absence of temporal decorrelation) and are obtained from Ω_{12} by letting the baseline length go to zero (i.e. $\alpha_z \rightarrow 0$).

Finding θ above determines the eigenvector \hat{p}_a and, assuming the eigenvectors are orthogonal (the forward scattering matrix is symmetric), \hat{p}_b as well, which enables simplification of (3). There are two methods for finding θ , since it appears in both T_{11} and Ω_{12} . One method relies on polarimetry alone, one on polarimetric interferometry. From polarimetry alone, finding θ is equivalent to pre- and post-multiplying the measured T_{11} by $R(-2\theta')T_{11}R(2\theta')$ and finding the θ' which gives a matrix of the form (7), in which case $\theta' = \theta$. From polarimetric interferometry, θ can be determined from the \underline{w}_1 and \underline{w}_2 which optimize γ in (4) [2]. Once θ is found, the following three vectors corresponding to co- and cross-polarization in the \hat{p}_a - \hat{p}_b basis (indicated by $p_a p_a$, $p_b p_b$, and $p_a p_b$) can be calculated by rotating \underline{w}_{HH} , \underline{w}_{VV} , and \underline{w}_{HV} by $R(2\theta)$:

$$\underline{w}_{p_a p_a} = \frac{1}{\sqrt{2}} \begin{pmatrix} 1 \\ -\cos 2\theta \\ \sin 2\theta \end{pmatrix} \quad \underline{w}_{p_b p_b} = \frac{1}{\sqrt{2}} \begin{pmatrix} 1 \\ \cos 2\theta \\ -\sin 2\theta \end{pmatrix} \quad \underline{w}_{p_a p_b} = \begin{pmatrix} 0 \\ \sin 2\theta \\ \cos 2\theta \end{pmatrix} \quad (11)$$

By using $\underline{w}_{p_a p_a}$, $\underline{w}_{p_b p_b}$, and $\underline{w}_{p_a p_b}$ in (4), with Ω_{12} from (6), three complex polarimetric interferometric coherences can be expressed in terms of four parameters. This can also easily be seen by equivalently extracting the co- and cross-polar terms, ($p_a p_a$, $p_b p_b$, and $p_a p_b$) in (3), yielding three cross-correlation equations, each of which are similar to the randomly-oriented cross-correlation in (1):

$$\begin{aligned} \frac{\langle E_{aa}(\vec{R}_1) E_{aa}^*(\vec{R}_2) \rangle}{\sqrt{\langle E_{aa}^2(\vec{R}_1) \rangle \langle E_{aa}^2(\vec{R}_2) \rangle}} &\propto e^{i\phi_0(z_0)} \int_0^{h_v} e^{i\alpha_z z} \exp\left[\frac{-2\sigma_{x_a}(h_v - z)}{\cos \theta_0}\right] dz \\ \frac{\langle E_{bb}(\vec{R}_1) E_{bb}^*(\vec{R}_2) \rangle}{\sqrt{\langle E_{bb}^2(\vec{R}_1) \rangle \langle E_{bb}^2(\vec{R}_2) \rangle}} &\propto e^{i\phi_0(z_0)} \int_0^{h_v} e^{i\alpha_z z} \exp\left[\frac{-2\sigma_{x_b}(h_v - z)}{\cos \theta_0}\right] dz \\ \frac{\langle E_{ab}(\vec{R}_1) E_{ab}^*(\vec{R}_2) \rangle}{\sqrt{\langle E_{ab}^2(\vec{R}_1) \rangle \langle E_{ab}^2(\vec{R}_2) \rangle}} &\propto e^{i\phi_0(z_0)} \int_0^{h_v} e^{i\alpha_z z} \exp\left[\frac{-(\sigma_{x_a} + \sigma_{x_b})(h_v - z)}{\cos \theta_0}\right] dz \end{aligned} \quad (12)$$

where $E_{aa}(\vec{R}_1)$ is the signal derived at end 1 of the baseline for transmit and receive polarization \hat{p}_a , and similarly for $E_{bb}(\vec{R}_1)$ and $E_{ab}(\vec{R}_1)$. The estimation of vegetation height

(h_v) and topography (z_0) is now schematically described by

$$\begin{pmatrix} h_v \\ z_0 \\ \sigma_{x_a} \\ \sigma_{x_b} \end{pmatrix} = M^{-1} \begin{pmatrix} A_{aa} \\ \phi_{aa} \\ A_{bb} \\ \phi_{bb} \\ A_{ab} \\ \phi_{ab} \end{pmatrix} \quad (13)$$

where A_{aa} is the amplitude of the first expression in (12) and ϕ_{11} is its phase. Eq. (13) shows that the required 4 parameters describing the oriented volume, including the two structure parameters h_v and z_0 , can be determined by the 6 observations provided by fully polarimetric interferometry *on a single baseline*. Qualitatively, the parameter estimation is enabled because the difference of the extinction coefficients of the eigenpolarizations effectively provides different penetrations into the vegetation, yielding different interferometric outcomes for the same vegetation canopy.

Figure 2 shows the calculated error of the vegetation height parameter, for a 20-m vegetation layer, as a function of the extinction coefficient difference between the eigenpolarizations $\sigma_{x_a} - \sigma_{x_b}$. The incidence angle is 35° , the wave length is 5.6 cm, the number of looks is 1000 ($\approx 100 - m^2$ area), and radar altitude is 8 km, typical of TOPSAR conditions. Figure 2 suggests that, for extinction coefficient differences greater than 0.1 db/m, single-baseline fully polarimetric interferometry can be used to determine the height of oriented vegetation volumes. Extinction coefficient differences of forest vegetation layers seem to be in the range of 0 to 0.2 db/m at P- through C-band [10,11], but the data on forest extinction coefficient differences due to vegetation orientation are scarce. From Figure 2, extinction coefficient differences of the order of those observed enable single-baseline height determination errors < 6 m. These single-baseline errors can be smaller than those obtained from two-baseline height estimation of randomly oriented volumes, shown by the horizontal line [6].

IV. Summary and Future Directions

This communication has demonstrated one example by which vegetation oriented structure can be measured with polarimetric interferometry. It has been shown that the height and underlying topography of an oriented vegetation layer can be determined with fully polarimetric interferometry by first optimizing the polarimetric or polarimetric interferometric coherence to find the eigenpolarizations of the oriented vegetation. The reduced parameter set characteristic of the eigenpolarizations is then estimated from interferometry done at the co- and cross-polar combinations of the eigenpolarizations. From (13), it can be seen that

if the eigenpolarizations were in the H and V directions, as may well be the case for a fair fraction of the Earth's vegetation, then the height, topographic, and extinction properties could be estimated without an HV cross-pol capability, or, similarly, with HH and HV alone. This will have applications to missions which do not have fully polarimetric interferometry, but will require the assumption that the eigenpolarizations are in the H and V directions. The actual distribution of the eigenpolarization vectors over all of the Earth's vegetation is not known.

Future work entails demonstrating the capability of single-baseline height determination when oriented volumes dominate the radar data, developing and maximizing the capability of polarimetric interferometry to characterize oriented volumes over tilted ground surfaces. It is anticipated that this may again involve some combination of optimizing polarimetric interferometric coherences, followed by estimation of a restricted set of parameters.

Acknowledgment

The research described in this paper was carried out by the Jet Propulsion Laboratory, California Institute of Technology, under contract with the National Aeronautics and Space Administration. The authors wish to acknowledge the financial support of the Office of Naval Research through NICOP award N8-53.

References

- [1] R. H. Waring, J. Way, R. Hunt Jr., , Morrissey, L., Ranson, K. J., Weishampel, J. F., Oren, R., and Franklin, S.E., "Imaging Radar for Ecosystem Studies," *BioScience*, vol. 45, pp. 715-723, 1995.
- [2] S. R. Cloude and K. P. Papathanassiou, "Polarimetric SAR Interferometry", *IEEE Trans. Geosci. Remote Sensing*, in press, 1998.
- [3] R. N. Treuhaft, S. N. Madsen, M. Moghaddam, and J. J. van Zyl, "Vegetation Characteristics and Surface Topography from Interferometric Radar," *Radio Science*, vol. 31, pp. 1449-1485, 1996.
- [4] W. M. Boerner, M. B. El-Arini, C. Y. Chan, P. M. Mastoris, "Polarization Dependence in Electromagnetic Inverse Problems," *IEEE Trans. Ant. and Prop.*, vol. AP-29, pp. 262-271, 1981.

- [5] J. J. van Zyl, H. A. Zebker, and C. Elachi, Imaging radar polarization signatures: Theory and observations, *Radio Science*, vo. 22, pp. 529-543, 1987.
- [6] R. N. Treuhaft, "The Vertical Structure of Vegetated Land Surfaces from Interferometric and Polarimetric Radar", in preparation, 1998.
- [7] R. N. Treuhaft, M. Moghaddam, and B. J. Yoder, "Forest Vertical Structure from Multi-baseline Interferometric Radar for Studying Growth and Productivity," *Proc. IGARSS97*, Singapore, pp. H6-06, 1997.
- [8] L. Tsang, J. A. Kong, and R. T. Shin, *Theory of Microwave Remote Sensing*, Wiley and Sons, New York, p. 460, 1985.
- [9] S. R. Cloude, and E. Pottier, "A Review of Target Decomposition Theorems in Radar Polarimetry," *IEEE Trans. Geosci. and Rem. Sens.*, vol. 34, pp. 498-518, 1996.
- [10] Y. Kuga, M. W. Whitt, K. C. McDonald, and F. T. Ulaby, "Scattering Models for Distributed Targets," in *Radar Polarimetry for Geoscience Applications*, ed. F. T. Ulaby and C. Elachi, Artech House, Inc., Norwood, MA, pp. 182-183, 1990.
- [11] E. S. Kasischke, M. Dobsen, D. Beverstock, and K. C. McDonald, "X and C-Band Forest Extinction Study," internal technical report, *Environmental Research Institute of Michigan, Ann Arbor*, 1989.

Figures

Figure 1: Schematic propagation of eigenpolarizations, showing different wavelength (refractivity) and attenuation (extinction coefficient) characteristics.

Figure 2: The 1-baseline calculated vegetation height parameter estimate error, for a 20-m oriented vegetation layer, as a function of the extinction coefficient difference between the eigenpolarizations generated by the vegetation orientation. The characteristics of the calculation are described in section III. The horizontal line is the 2-baseline interferometric height parameter estimate accuracy for a randomly oriented volume.

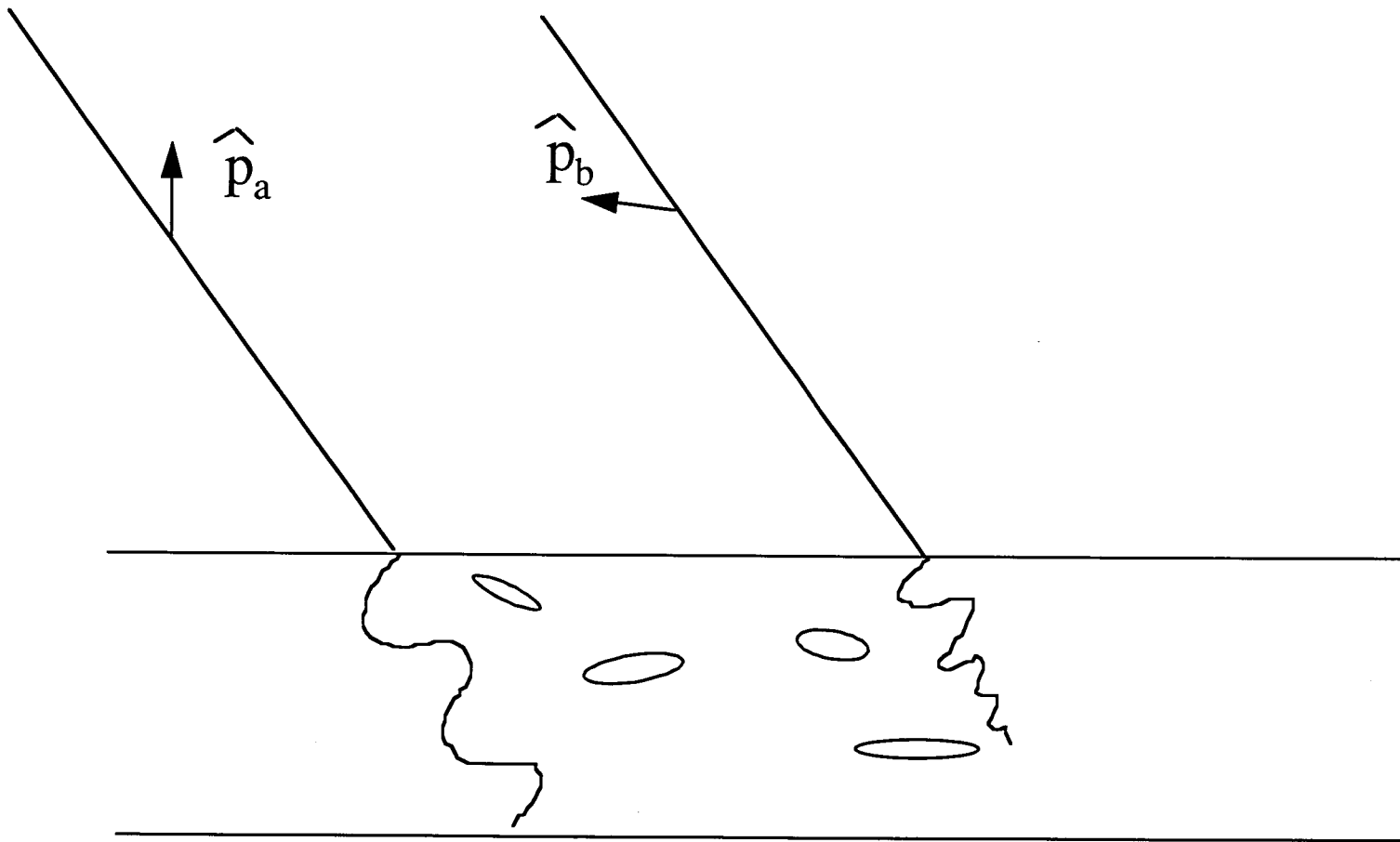


Figure 1

Figure 2

